SIMULATION OF HETEROGENEOUS AZEOTROPIC DISTILLATION PROCESS WITH A NON-EQUILIBRIUM STAGE MODEL

Hitoshi Kosuge, Hamid Reza Mortaheb

Department of Chemical Engineering, Tokyo Institute of Technology,
12-1, Ookayama-2, Meguro-ku, Tokyo 152, Japan

ABSTRACT

A rate-based simulation method is developed with the correlation for mass transfer rate, which was obtained in our experiments of the homogeneous and heterogeneous ternary distillation with a sieve tray column. The simulation method is applied to the process of ethanol dehydration with benzene, which consists of a dehydration- and an entrainer recovery column. In the simulation study, the effect of tray specifications, reflux ratio, locations of feed and recycle streams, and recycle flow rate on separation performance of the process are investigated. The simulation results show that the top vapor concentration closer to the heterogeneous azeotrope of the system gives a more efficient separation.

INTRODUCTION

Heterogeneous azeotropic distillation is widely used to separate azeotropic mixtures. In the separation process of a binary azeotropic mixture, an entrainer is added to produce a binary azeotrope with one of the components in the mixture, or a ternary heterogeneous azeotrope with both of them. Since in the latter case the whole concentration region is divided into several regions by the distillation boundaries, the distillation column is sometimes operated in a narrow distillation region so that the target component is separated from the original mixture. To operate the distillation column successfully in this region, precise prediction of the separation performance of the column is required using a proper design model, otherwise undesired separation may occur.

In design of tray columns for the heterogeneous distillation, an equilibrium stage model is often used. However, it may be difficult to predict the exact concentration profile in the column, because the equilibrium stage model does not consider the liquid phase mass transfer resistance, of which the effect on the separation performance of the column cannot be neglected in two-liquid region [1]. Krishnamurthy and Taylor [2,3,4] also showed that the predicted concentrations by the nonequilibrium model are largely different from those by the equilibrium stage

model with tray efficiencies, and they pointed out that the difference was caused by the difference in mass transfer resistances and the diffusional interaction effects.

In our previous works [1,5,6], the correlations of mass transfer rates and clear liquid height in the sieve tray were obtained in the experiments of homogeneous and heterogeneous distillation with a sieve tray column. A non-equilibrium stage model was then developed to predict the separation performance of the sieve tray column in the homogeneous and heterogeneous distillation at total reflux conditions. In this paper, a simulation procedure based on the non-equilibrium stage model is developed for a heterogeneous azeotropic distillation process, and is applied to the ethanol dehydration process consisting of a dehydration- and an entrainer recovery column, to study the effect of operating conditions on the separation performance of the two distillation columns.

SIMULATION MODEL

Non-equilibrium Stage Model

In our previous experiments of heterogeneous distillation with the ethanol-benzene-water system, froth regime was observed on the tray in whole the two-liquid region, and the external appearance of the fluid was cloudy emulsion [1]. This may indicate that the small bubbles and droplets are well mixed with the continuous liquid. Therefore, mass transfer on the tray is expected to occur between the vapor and organic phases, the vapor and aqueous phases, and the organic and aqueous phases. Since, however, the observed concentrations of two liquids on the tray in the experiments were close to the equilibrium conditions, two liquids were assumed to be in equilibrium each other. Finally, mass and heat transfer between the vapor and each liquid phase is taken into account in simulation of the tray.

Table 1 summarizes the basic equations for simulation of each tray [1]. The clear liquid height of the tray is calculated by Eq. (1), and vapor phase diffusional rate per unit volume, that is, the vapor phase volumetric diffusion flux is calculated by Eq. (2). Both correlations were obtained in our previous experiments [1,6]. Eq. (3) expresses the vapor phase volumetric sensible heat flux obtained by the analogy between heat and mass transfer. Eq. (4) represents the vapor phase volumetric convective mass flux [7]. The liquid phase mass transfer coefficient is calculated by Eq. (8) [8], and liquid phase heat transfer coefficient, Eq. (10) is derived from the analogy between heat and mass transfer.

In simulation of each tray, clear liquid height is calculated by Eq. (1) with initial guess for the vapor flow rate at the tray, and then divided into a number of thin segments. In each segment, heat and mass transfer rates between the vapor and each liquid phase are calculated separately according to the following steps.

1) The concentrations and flow rate of each liquid phase are calculated from the overall liquid concentrations and flow rate at the inlet of the segment by using the liquid-liquid equilibrium calculation.

2) The liquid concentrations at the vapor-liquid interface, ω_{Lis}, are assumed, then the vapor concentrations and temperature at the interface, ω_{Gis} and T_s, are calculated by the vapor-liquid equilibrium calculation. The vapor phase volumetric diffusion fluxes, $J_{Gis}\,a$, sensible heat fluxes, q_{Gs}, convective mass fluxes, $\rho_{Gs}\,v_s\,a$, and mass

fluxes, N_{Gi} a, are calculated by Eqs. (2), (3), (4), (5) and their definitions, respectively. Then, liquid phase volumetric diffusion fluxes, J_{Lis} a, are calculated by Eq. (6) with the conditions of $N_{Li}=N_{Gi}$. The new liquid concentrations at the interface are calculated by the Newton-Raphson method, in which the objective functions are introduced based on Eqs. (7) and (8). These steps are repeated until convergence for ω_{Lis} is obtained.

3) The liquid bulk temperature is calculated by Eqs. (9) and (10) with the heat balance around the vapor-liquid interface, Eq. (11).

4) The overall flow rate and concentrations at the outlet of the segment are obtained from the overall and component mass balances, Eqs. (12) and (13), where the mass transfer rates of vapor and each liquid phase are assumed to be proportional to the height of that liquid in the segment. The heights of both liquids in the segment are calculated by Eqs. (14a) and (14b), where the fraction of liquid I in the total liquid, β, is obtained from liquid-liquid equilibrium based on the overall liquid concentrations in the segment.

5) The calculations from step 2 to 4 are repeated from top to bottom of the liquid on the tray. The details were shown elsewhere [1].

Table 1 Basic equations of simulation

Clear liquid height:

$$H_{CL} = 317.9\ H_W\ F^{-0.82}\ (\rho_G / \rho_{Lm})\ Re_G^{\ -0.48} \quad (1)$$

Vapor phase mass and heat transfer rates:

$$Sh_{Gi}\ a\ (J_{Gis}/N_{Gi})\ d_H = 0.012 Re_G^{\ 0.862}\ Sc_{Gis}^{\ 1/3}\ F^{1.2}\ (Fr/We) \quad (2)$$

$$Nu_G\ a\ d_H = 0.012\ Re_G^{\ 0.862}\ Pr_{Gs}^{\ 1/3}\ F^{1.2}\ (Fr/We) \quad (3)$$

$$\rho_{Gs}\ v_s\ a = \frac{\sum(-J_{Gis}\ a\ \lambda_i) - q_w\ a - q_G\ a}{\sum -\lambda_i\ \omega_{Gis}} \quad (4)$$

$$N_{Gi}\ a = J_{Gis}\ a + (\rho_{Gs}\ v_s\ a)\omega_{Gis} \quad (5)$$

Liquid phase mass and heat transfer rates:

$$J_{Lis}a = N_{Li}a - \sum(N_{Lj}a)\omega_{Lis} \quad (6)$$

$$J_{Lis}a = \rho_L k_{Li}a\ (\omega_{Lis} - \omega_{Li\infty}) \quad (7)$$

$$k_{Li}\ a = 19700\ D_{Lim}^{\ 0.5}\ (0.4 F_a + 0.17) \quad (8)$$

$$q_L a = h_L a (T_{L\infty} - T_s) \quad (9)$$

$$h_L\ a = 19700\ \alpha^{0.5}\ (\rho_L c_{pL})(0.4\ F_a + 0.17) \quad (10)$$

$$q_L a = q_G a - \sum \lambda_i N_{Gi} a \quad (11)$$

Overall and component mass balance:

$$\Delta V = \sum\ [(N_{Gi}\ a)^{I}\ z^{I} + (N_{Gi}\ a)^{II}\ z^{II}]\ A_b \quad (12)$$

$$\Delta(V\omega_{Gi}) = [(N_{Gi}a)^{I} z^{I} + (N_{Gi}a)^{II} z^{II}] A_b \quad (13)$$

$$\beta_m = \beta (M^{I}/M); \quad \beta_v = \frac{\beta_m / \rho_L^{\ I}}{\beta_m / \rho_L^{\ I} + (1-\beta_m)/\rho_L^{\ II}} \quad (14a)$$

$$z^{I} = z \times \beta_v; \quad z^{II} = z \times (1-\beta_v) \quad (14b)$$

The vapor-liquid and vapor-liquid-liquid equilibria of the system are estimated from the vapor pressures of pure components by the Antoine equation, and from the liquid phase activity coefficients by the UNIQUAC equation, where the Antoine constants and UNIQUAC parameters are taken from the literature [9]. The viscosity of the pure vapor is calculated from Chung et al. method and for vapor mixture Wilke's method is applied. The thermal conductivity of vapor and liquid mixtures are calculated using the methods of Chung et al. and Li, respectively. The surface tension of liquid mixture is calculated using the modified Macleod correlation. The vapor phase binary diffusion coefficient is estimated by the correlation of Fuller et al., and for estimation of the effective diffusion coefficients in the liquid phase the Perkins and Geankoplis equation is used [10].

Process Configuration

The schematic diagram of the heterogeneous azeotropic distillation process is shown in **Fig. 1**. A process consists of a dehydration column and an entrainer recovery column. An alcohol-water mixture with a concentration near its azeotrope, F_0, is fed to the dehydration column. The mixture of entrainer makeup and the recycle flow from the top of the entrainer recovery column, $F_{m,}$ is also fed to the column. The pure alcohol can be obtained from the bottom of the dehydration column as a product.

The overhead vapor is condensed and split into two liquid phases in the decanter.

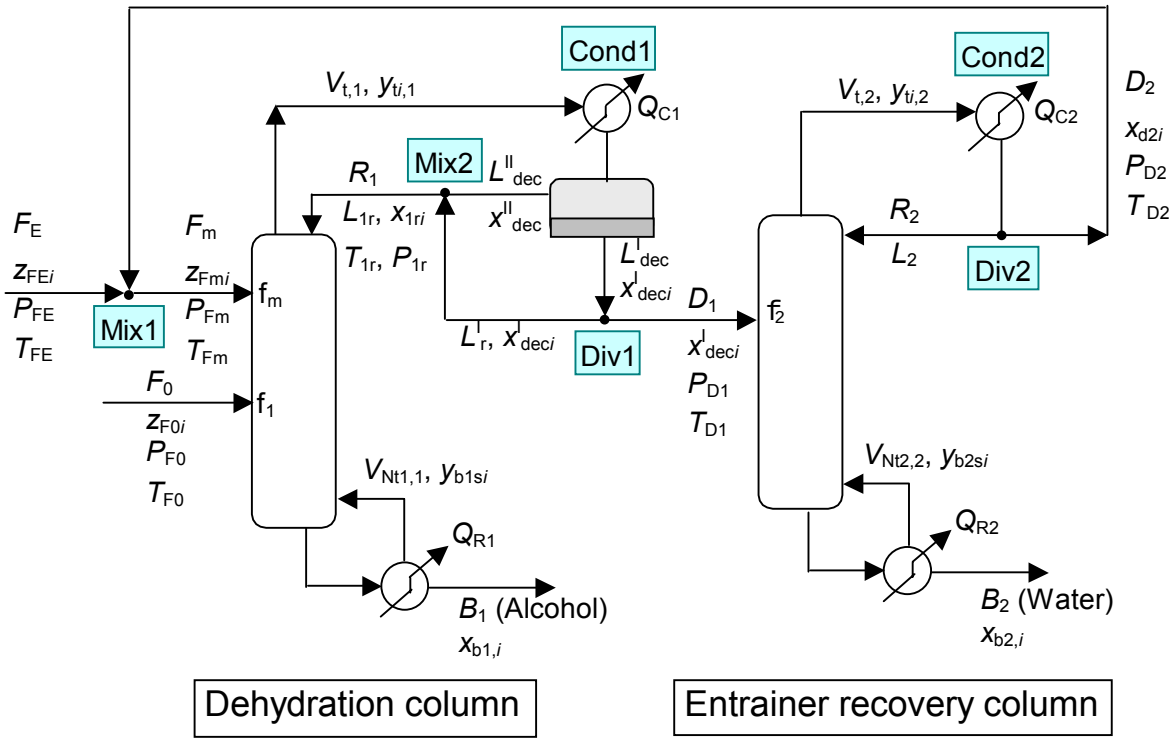

Fig. 1 Schematic diagram of heterogeneous azeotropic distillation process

The organic entrainer-rich phase is totally returned to the dehydration column, while the aqueous phase is fed to the entrainer recovery column. The feed of the second column is separated in the column into nearly pure water and an entrainer-rich mixture.

Calculation Procedure

The degree of freedom for a ternary system in the process shown in Fig. 1 is ($2N_{t1}$ + $2N_{t2}$ + 27). Then, Q_{Div1}, Q_{Div2}, Q_{Mix1}, Q_{Mix2}, Q_{Dec}, P_{D1}, P_{D2}, P_{Fm}, P_{1r}, $P_{out,Dec}$, $T_{out,Cond1}$ (= T_{Dec}), $T_{out,Cond2}$ (= $T_{saturated}$), N_{t1}, N_{t2}, f, f_m, f_2, $P_{j,1}$, $P_{j,2}$, $Q_{j,1}$, $Q_{j,2}$, F_0, z_{F0i}, z_{FEi}, T_{F0}, P_{F0}, T_{FE}, P_{FE}, R_1, and R_2, which are totally ($2N_{t1}$ + $2N_{t2}$ + 25), are specified. The entrainer and top product flow rates (F_E, D_1) can be specified as the two remained variables. In that case, however, the predicted concentrations of overhead vapor in the dehydration column may move out of the two-liquid region. When such a case occurs, the convergence of calculation becomes more difficult. Therefore, to avoid such a difficulty, the overhear vapor concentrations, $y_{ti,1}$, are specified as the remained two variables. Also, D_1/F_0 and F_E/F_0 are used as the independent variables in the simulation.

For the dehydration column, the concentrations and flow rate of reflux liquid, and the flow rate of overhead vapor are calculated from the estimated values of D_1/F_0 and F_E/F_0. The calculation is then carried out from top to bottom of the column (j = 2 to N_{t1} -1), where the calculation in each tray proceeds from top to bottom of the liquid by considering the mass transfer rates between vapor and liquids as mentioned above. In order to reduce the calculation time, the effect of liquid phase resistance is only considered in the calculations in the heterogeneous liquid region. Whether the liquid phase splitting occurs or not in the segment is examined by the modified tangent plane phase stability test proposed by Cairns and Furzer [11]. After the liquid and vapor flow rates, L_{Nt1-1}, V_{Nt1}, and their concentrations, $x_{Nt1-1,i}$, $y_{Nt1,i}$, at the bottom of the column (j = N_{t1}-1) are obtained, the vapor concentrations, y_{b1si}, in equilibrium with the bottom concentrations are calculated, and compared with the vapor concentrations at the bottom of the column, $y_{Nt1,i}$. If the convergence condition is not satisfied, the calculations are repeated with new values for D_1/F_0 and F_E/F_0, which are estimated by the Newton-Raphson method with the following objective functions:

$$f_i(D_1/F_0, F_E/F_0) = y_{b1si} - y_{Nt1,i} \quad (i = 1, 2) \qquad (15)$$

where the required partial derivatives for the calculations are obtained numerically, and the new values of the independent variables may be determined by applying a damping factor to avoid the numerical oscillation.

For the entrainer recovery column, the flow rates of reflux liquid and overhead vapor are obtained from the overall material balance around the column. If the concentrations of the top product, x_{d2i}, are estimated, the concentrations of the bottom product, x_{b2i}, are obtained by component material balance around the column. Once the flow rates and concentrations of both vapor and liquid streams above the top tray of the entrainer recovery column are known, the distillation calculation is carried out from top to bottom of the column (j = 2 to N_{t2} -1) using the segment-by-segment method. After the liquid and vapor flow rates, L_{Nt2-1}, V_{Nt2}, and their concentrations, $x_{Nt2-1,i}$, $y_{Nt2,i}$ at the bottom of the column (j = N_{t2}-1) are obtained, the liquid concentrations, x_{b2si}, in equilibrium with the bottom vapor are calculated, and compared with the bottom liquid concentrations, x_{b2i}. If convergence condition is not satisfied, the calculations are repeated with new values for x_{d2i}, where the new values of x_{d2i} are estimated by the Θ-method.

The computing time depends on the accuracy specified for the convergence condition. For example, the calculation takes about 10 seconds per tray for an

accuracy of 1×10^{-4} with a personal computer of 800 MHz CPU. More information about the calculation procedures and the developed software can be found elsewhere [12].

Specifications in the Simulation

The specifications of the columns and main operating conditions in the present simulation are summarized in **Table 2**. The sizes of columns are selected similar to the experimental column in the previous research [1]. The feed flow rate, F_0, is set within the operating capacity of the column. The columns operate under atmospheric pressure, and the pressure drops in all equipment are assumed to be negligible. The number of trays in the entrainer recovery column is fixed.

EFFECT OF TRAY SPECIFICATIONS ON SEPARATION PERFORMANCE

The separation performance of the heterogeneous azeotropic column is simulated by varying the tray specifications including free area and weir height. **Figure 2(a)** shows the effect of free area of the trays on the concentration profile in the dehydration column. The concentration profile of ethanol goes toward the pure ethanol more rapidly as free area of the trays increases. This is due to increase of vapor-liquid interfacial area on the trays by increasing free area, which enhances mass transfer rate. In order to obtain the number of trays required for a specified purity of ethanol at the bottom of the dehydration column, the simulation is carried out with the same

Table 2 Main specifications of the columns in present simulation

Dehydration Column:

Column inner diameter = 0.046 m Tray hole diameter = 0.0015 m
Tray bubbling area = 0.00212 m^2 Column pressure = 1 atm
Decanter temperature = 298.15 K Wall heat flux = 0 W/m^3
Feed flow rate = 5.42 mol/hr
Feed: z_{F01}=0.89, z_{F03}=0.11, P_{F0}=1 atm, T_{F0}=bubble point
Entrainer: z_{Fm2}=1.00, P_{Fm}=1 atm, T_{Fm}=298.15K

Entrainer Recovery Column:

Column inner diameter = 0.046 m Tray hole diameter = 0.0015 m
Tray bubbling area = 0.00212 m^2 Column pressure = 1 atm
Wall heat flux = 0 W/m^3
Number of trays = 10

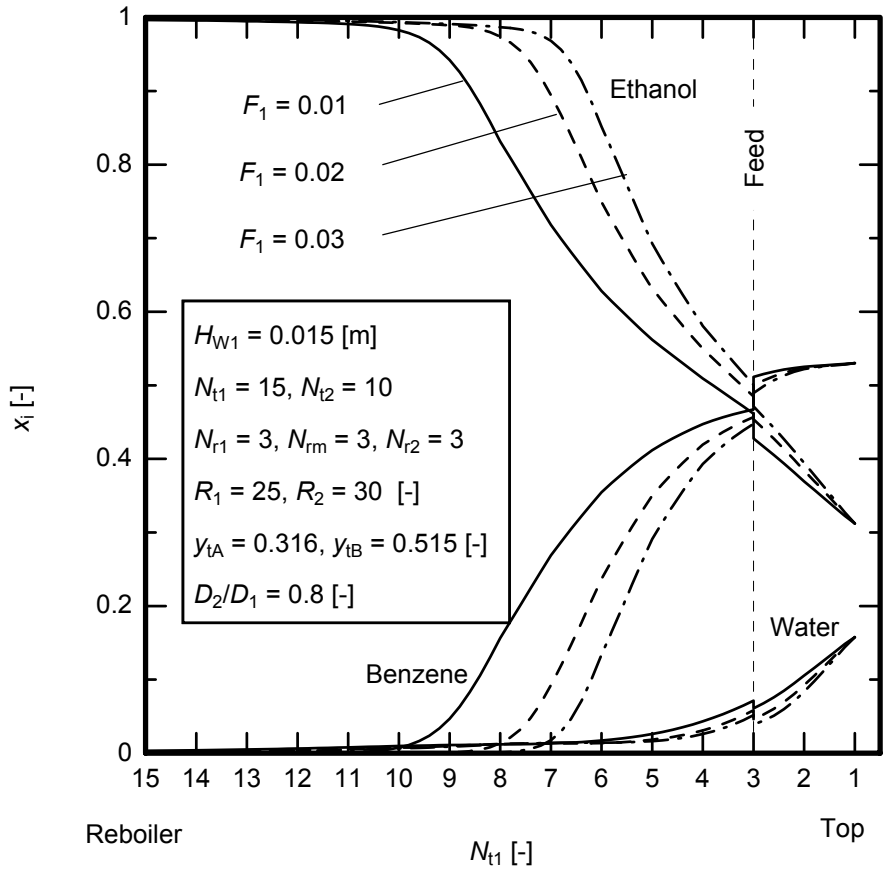

*Fig. 2(a) Effect of free area of trays on concentration profiles in the dehydration colum*n

conditions as in Fig. 2(a) except for the number of trays in the column, which is considered sufficiently large for the separation. **Figure 2(b)** shows that the number of trays required to meet the 99.9% ethanol at the bottom decreases rapidly by increasing free area of the trays. On the other hand, simulation of separation performance by varying weir height of the trays in the dehydration column shows that the number of trays required in the dehydration column to obtain ethanol with the specified purity decreases by increasing weir height, as shown in **Fig. 3**. This is for the reason that increase of weir height increases clear liquid height, and subsequently the overall mass transfer between the contacting phases on the tray increases.

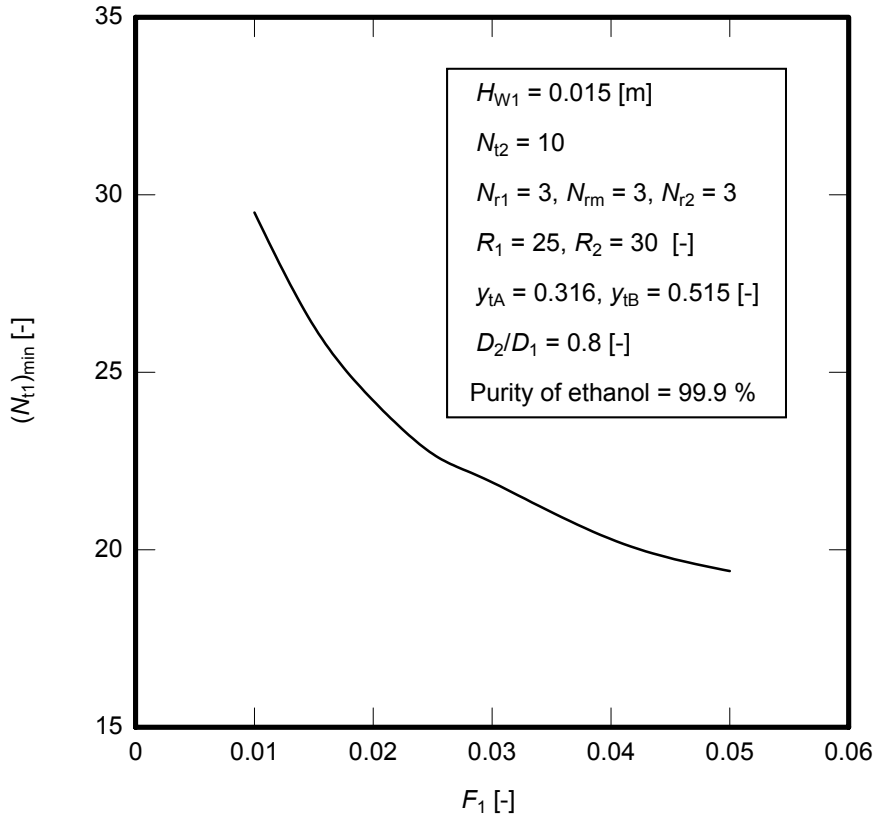

Fig. 2(b) Effect of free area on required number of trays in the dehydration column

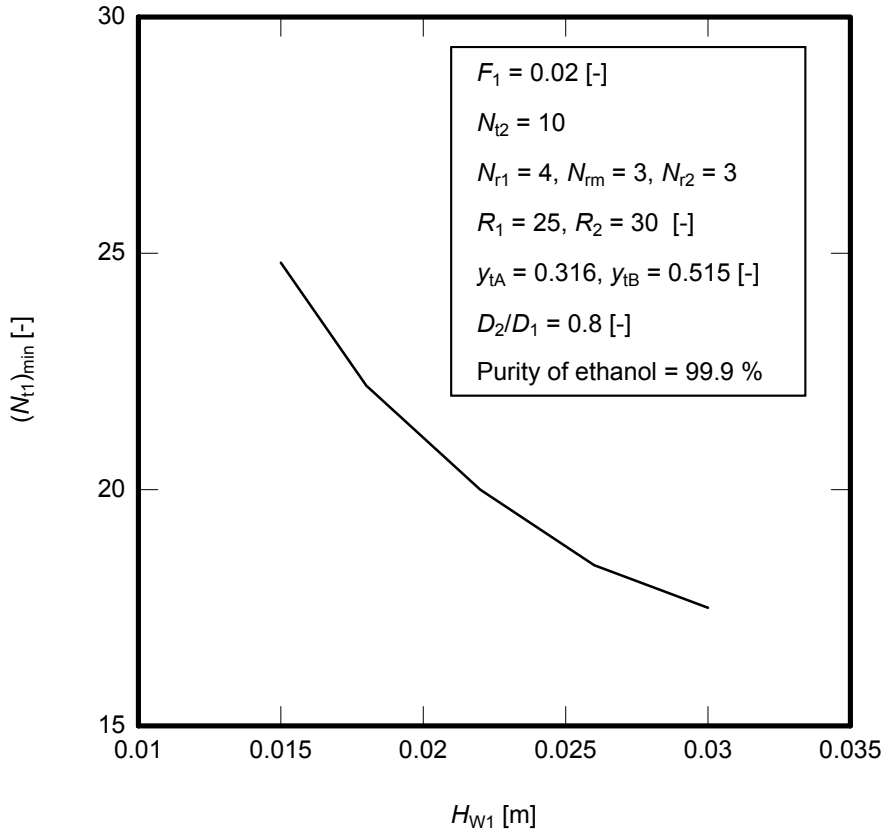

Fig. 3 Effect of weir height on required number of trays in the dehydration column

EFFECT OF OPERATING PARAMETERS ON SEPARATION PERFORMANCE

Effect of Reflux Ratio

The effect of reflux ratio in the dehydration column on the distillation path is shown in **Fig. 4(a)**. Since the operable range of reflux ratio under the given specifications is from 18 to 50, the distillation paths with the reflux ratios18, 25,and 50 are shown in the figure. The path approaches the ethanol-benzene edge as the reflux ratio increases, that is, the bottom product approaches the pure ethanol with a fewer number of trays. However, as shown in **Fig. 4(b)**, the number of trays required obtaining ethanol with the specified purity decreases slightly by increasing the reflux ratio after a sharp decrease around reflux ratios of 18 to 25. This is because the clear liquid heights on the trays decrease in the higher reflux ratios due to higher vapor velocity in the column, and then the overall mass transfer on the trays decreases.

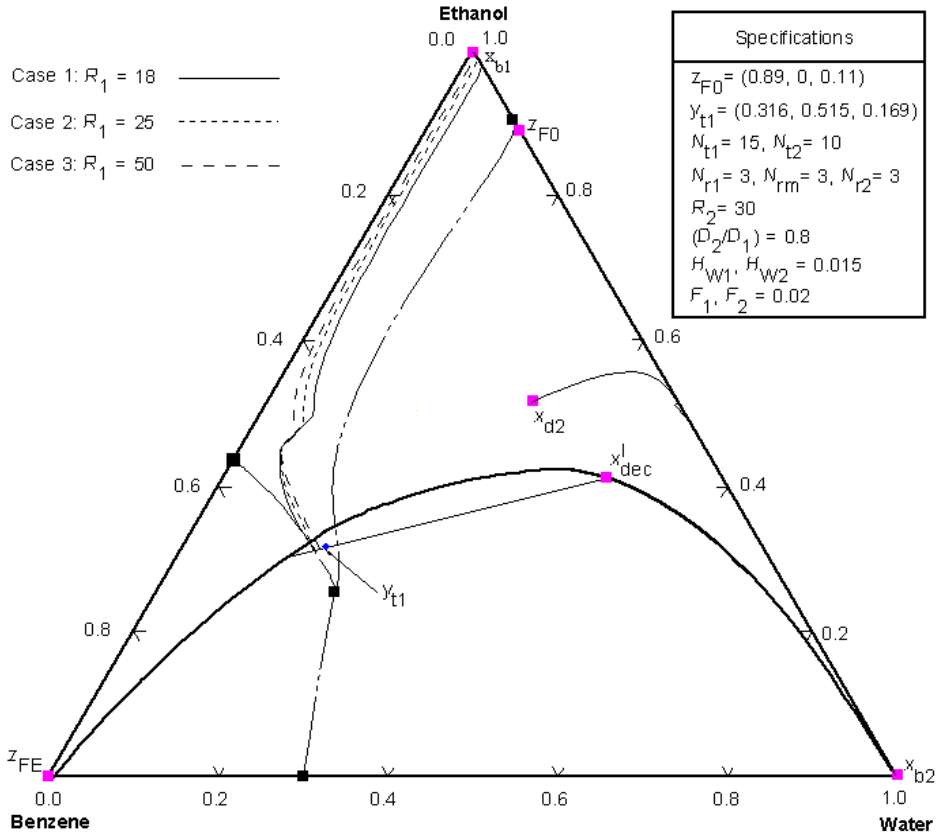

Fig. 4(a) Effect of reflux ratio on distillation path in the dehydration column

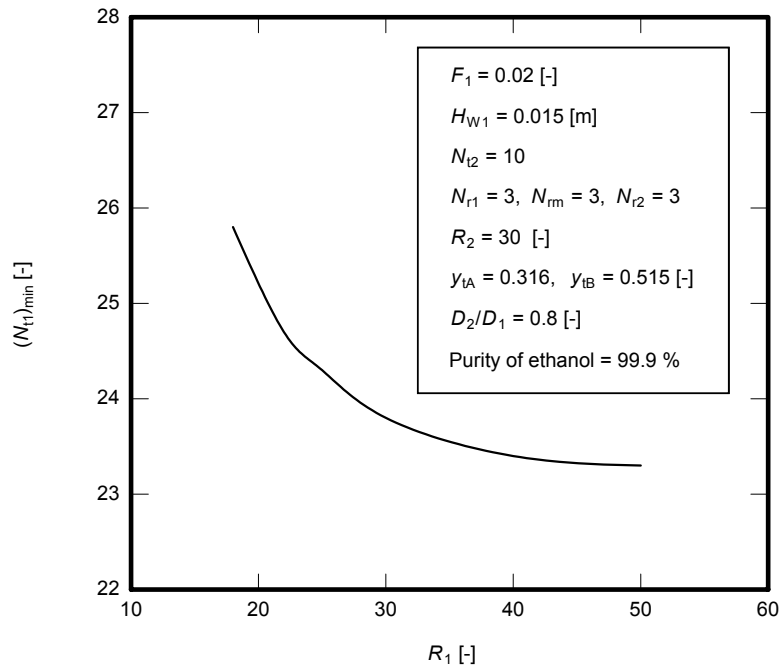

Fig. 4(b) Effect of reflux ratio on required number of trays in the dehydration column

Effect of Feed and Recycle Stream Locations

Figure 5(a) shows the liquid concentration profiles in the dehydration column for various feed locations with the same other conditions. The figure shows that the concentration gap at the feed point becomes smaller as the feed location is set downward. **Figure 5(b)** shows the effect of feed location on the minimum number of trays to meet the specified purity of ethanol at the bottom of the dehydration column. More trays are required as the feed location is set downward. However, the required number of trays becomes almost constant for lower feed trays than 9^{th} stage.

On the other hand, a similar effect was found by varying the location of recycle stream between stages 2 to 9. This indicates that the number of trays required to obtain ethanol product with the specified purity increases as the location of recycle stream is set downward. As a result, the location of both feed and recycle streams should be selected close to the top of the column for a more efficient separation.

Effect of Recycle Flow Rate

The separation performances of both dehydration and entrainer recovery columns are affected by varying the recycle flow rate from the entrainer recovery column to the dehydration column. **Figure 6** shows the effect of recycle flow rate on the distillation paths in both columns. As expected from the overall material balance around the entrainer recovery column, by increasing the recycle flow rate, D_2/D_1, the concentration of top product of the entrainer recovery column, $x_{d2,1}$ to $x_{d2,4}$, becomes close to the feed concentration of this column, x^{l}_{dec}. Meanwhile the concentration of bottom product, $x_{b2,1}$ to $x_{b2,4}$, goes toward the water vertex that results in better recovery of entrainer in the entrainer recovery column. Increase of the recycle flow rate also increases the liquid and vapor flow rates in the dehydration column, and shifts the concentration profile in the dehydration column toward the ethanol-benzene edge. Consequently, the number of trays required to obtain the specified purity of ethanol at the bottom of dehydration column decreases with increase of recycle flow rate.

Effect of Overhead Vapor Concentration

The separation performance of the columns was simulated with varying the overhead vapor concentration of the dehydration column. **Figure 7** shows that as the overhead vapor concentration becomes close to the ternary heterogeneous azeotrope, the concentration of the top product of the dehydration column, $x^{l}_{dec,1}$ to $x^{l}_{dec,4}$, moves toward the water vertex on the binodal curve, and the concentration of top product of

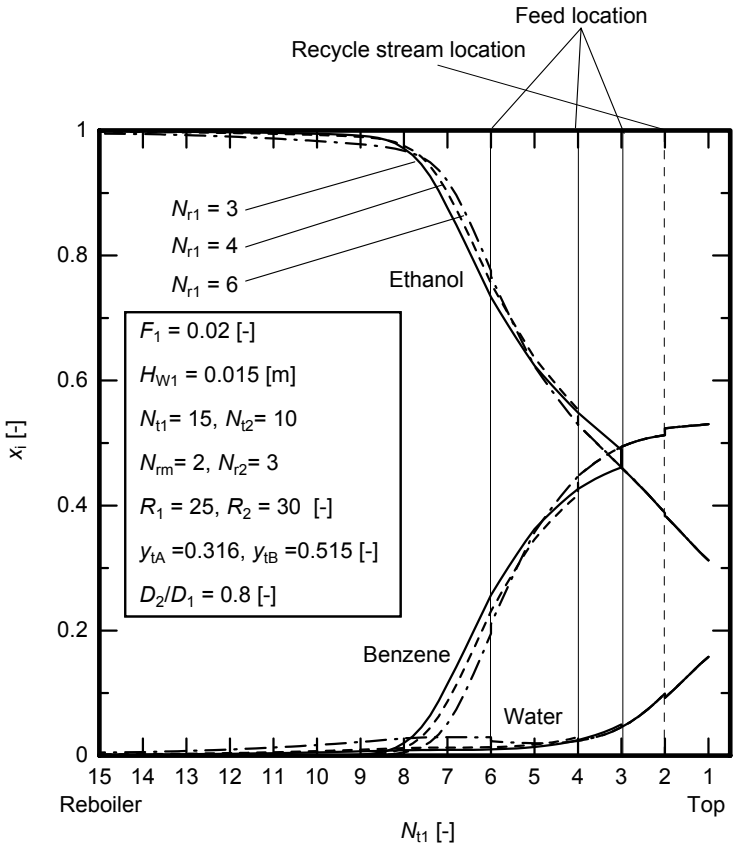

Fig. 5(a) Effect of feed location on concentration profiles in the dehydration column

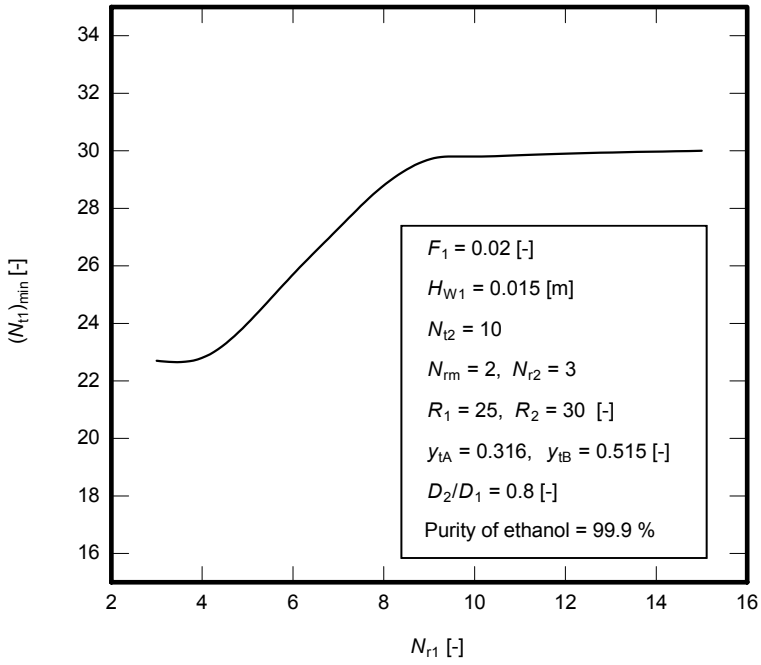

Fig. 5(b) Effect of feed location on required number of trays in the dehydration column

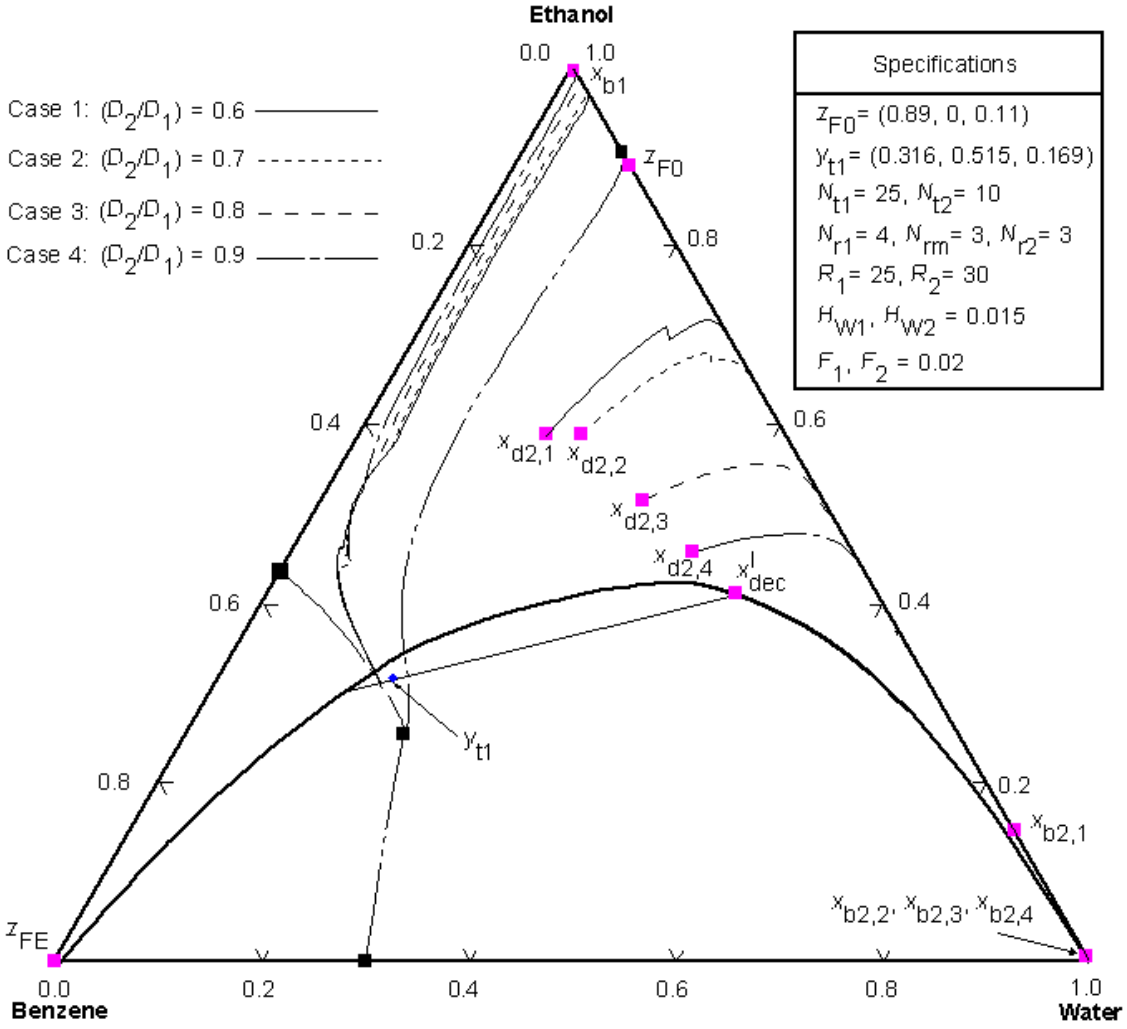

Fig. 6 Effect of recycle flow rate on distillation paths in the process

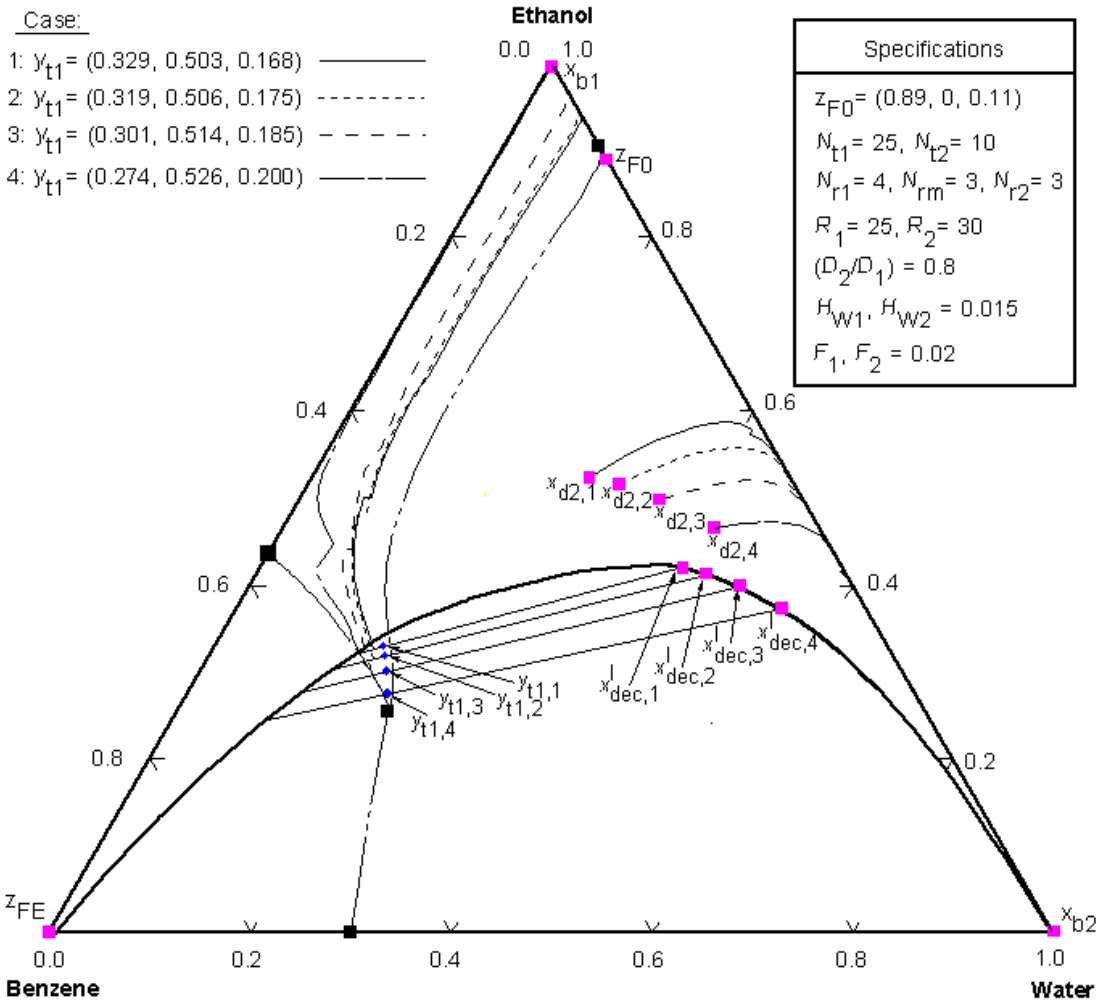

Fig. 7 Effect of overhead vapor concentration on distillation paths in the process

the entrainer recovery column, $x_{d2,1}$ to $x_{d2,4}$, also becomes close to the water vertex. At the same time, the distillation path in the dehydration column approaches the distillation boundary between the ternary heterogeneous azeotrope and ethanol-benzene azeotrope and goes toward the ethanol-benzene edge along the distillation boundary. Therefore, separation of ethanol in the dehydration column is more effective for a closer overhead vapor concentration to the ternary heterogeneous azeotrope. **Figure 8** shows that the number of trays required to obtain the specified purity of ethanol at the bottom of the dehydration column decreases greatly as the vapor concentration goes toward the ternary heterogeneous azeotrope.

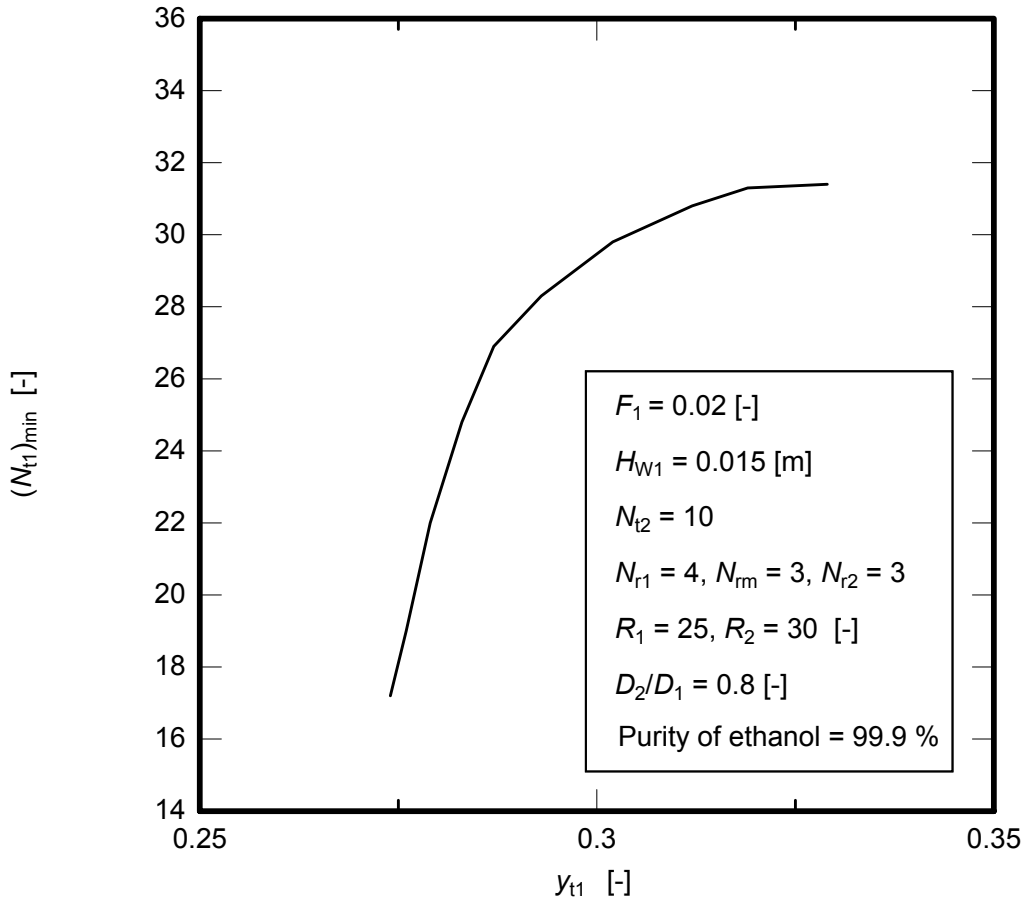

Fig. 8 Effect of overhead vapor concentration of required number of trays in the dehydration column

CONCLUSION

A simulation procedure for prediction of separation performance in a heterogeneous azeotropic distillation process that consists of a dehydration column and an entrainer recovery column is developed based on the mass transfer model. Dehydration of the ethanol-water mixture with benzene was studied as a typical example. Based on the

simulation results, the following conclusions are obtained:

1) The enhancement in the separation performance of the process by increasing free area and weir height of the trays can be predicted by the present non-equilibrium model. This represents an advantage of the non-equilibrium stage model compared with the equilibrium model.
2) The effects of operating parameters on separation performance are analyzed in terms of the concentration profile along the column. Among the operating parameters, as the recycle flow rates from the entrainer recovery column increase, the number of trays in dehydration column decrease, and the purity of the bottoms product of the entrainer recovery column increases.
3) As the concentrations of the overhead vapor in the dehydration column approach the ternary heterogeneous azeotrope, the number of the dehydration column decreases, and also the separation performance of the entrainer recovery column is enhanced. The latter result implies that the number of trays in the entrainer recovery column decrease.

NOMENCLATURE

A_b	=	bubbling area of tray	[m^2]
A_h	=	total area of holes	[m^2]
a	=	interfacial area per unit volume of liquid on tray	[m^2/m^3]
B	=	bottom product flow rate	[kmol/hr]
c	=	number of components	[-]
c_p	=	specific heat	[J/(kg K)]
D	=	top product flow rate	[kmol/hr]
D_{im}	=	effective diffusion coefficient of component i	[m^2/s]
d_H	=	hole diameter	[m]
F	=	free area of tray {=A_h/A_b}	[-]
F_0	=	feed flow rate	[kmol/hr]
F_a	=	vapor phase F-factor {=$U_a \rho_G^{0.5}$}	[$kg^{0.5}/(m^{0.5}$ s)]
F_E	=	entrainer flow rate	[kmol/hr]
F_m	=	flow rate of entrainer and recycle streams mixture	[kmol/hr]
f	=	feed location	[-]
f_m	=	recycle flow location	[-]
Fr	=	Froude number {=$U_a^2/(g\ H_{CL})$}	[-]
g	=	gravity acceleration	[m/s^2]
H_{CL}	=	clear liquid height on tray	[m]
H_W	=	weir height	[m]

h_L	=	molar enthalpy of liquid phase	[kJ/kmol]
J_{Gis}	=	vapor phase diffusion flux	[kg/(m^2 s)]
k_L	=	liquid phase mass transfer coefficient	[m/s]
L_{1r}	=	reflux flow rate of dehydration column	[kmol/hr]
L_2	=	reflux flow rate of entrainer recovery column	[kmol/hr]
L^l_r	=	flow rate of aqueous phase recycled to dehydration column	[kmol/hr]
M	=	mean molecular weight based on overall liquid concentrations in segment	[kg mol^{-1}]
M^l	=	mean molecular weight of liquid l in segment	[kg mol^{-1}]
N_D	=	degree freedom	[-]
N_{Gi}	=	vapor phase mass flux	[kg/(m^2 s)]
N_t	=	total number of stages in column	[-]
$(N_{t1})_{min}$	=	number of stages required in dehydration column to obtain a specified purity of ethanol	[-]
Nu_G	=	vapor phase Nusselt number {$=q_G d_H / \kappa_{Gs}(T_s - T_\infty)$}	[-]
N_r	=	number of stages in rectifying section	[-]
N_{rm}	=	number of stages above recycle flow	[-]
P	=	pressure	[atm]
Pr_{Gs}	=	vapor phase Prandtl number {$=c_{pGs}\,\mu_{Gs}/\kappa_{Gs}$}	[-]
Q	=	heat loss	[kW]
Q_C	=	condenser duty	[kW]
Q_R	=	reboiler duty	[kW]
q_G	=	vapor phase sensible heat flux	[W/m^2]
q_w	=	wall heat flux	[W/m^2]
R	=	reflux ratio	[-]
Re_G	=	vapor-phase Reynolds number based on vapor velocity at hole {$=\rho_G U_h d_H/\mu_G$}	[-]
Sc_{Gis}	=	Schmidt number {$=\mu_{Gs}/\rho_{Gs} D_{Gim}$}	[-]
Sh_{Gi}	=	Sherwood number {$=\dfrac{N_{Gi} d_H}{\rho_{Gs} D_{Gim} \Delta \omega_{Gi}}$}	[-]
T	=	temperature	[K]
U_a	=	vapor velocity base on bubbling area	[m/s]

U_h	= vapor velocity at hole	[m/s]
V	= vapor mass flow rate	[kg/s]
V_t	= overhead vapor flow rate	[kmol/hr]
We	= Weber number $\{=\rho_G U_a^2 d_H/\sigma\}$	[-]
x	= liquid phase mole fraction	[-]
x_{1ri}	= concentration of reflux liquid in dehydration column	[-]
y	= vapor phase mole fraction	[-]
y_{ti}	= overhead vapor concentration	[-]
z	= segment height	[m]
z_{F0i}	= concentration of main feed	[-]
z_{FEi}	= concentration of entrainer feed	[-]
z_{Fmi}	= concentration of mixture of entrainer and recycle streams	[-]

<*Greek letters*>

α	= thermal diffusivity $\{=\kappa_L/\rho_L c_{pL}\}$	[m^2/s]
β	= fraction of liquid I in total liquid in segment, on mole basis, calculated from liquid-liquid equilibrium	[-]
β_m	= fraction of liquid I in total liquid in segment, on mass basis	[-]
β_v	= fraction of liquid I in total liquid in segment, on volume basis	[-]
$\Delta\omega_{Gi}$	= vapor phase concentration driving force	[-]
κ	= thermal conductivity	[W/(m K)]
λ	= latent heat of vaporization	[J/kg]
μ_G	= vapor phase viscosity	[Pa s]
v_s	= normal component of interfacial velocity	[m/s]
ρ	= density	[kg/m^3]
σ	= liquid surface tension	[N/m]
ω	= mass fraction	[-]

< *Subscript and Superscript* >

1	=	dehydration column
2	=	entrainer recovery column
A	=	most volatile component (=ethanol)
B	=	intermediate component (=benzene)
b	=	bottom condition
dec	=	decanter
F0	=	main feed
FE	=	entrainer
G	=	vapor phase
i	=	component *i*
j	=	stage number
L	=	liquid phase
m	=	mass fraction average
s	=	vapor-liquid interface
t	=	top condition
∞	=	bulk condition
I	=	liquid phase I
II	=	liquid phase II

LITERATURE CITED

1. H. R. Mortaheb, H. Kosuge and K. Asano (2002), to be published in Chem. Eng. J.

2. R. Krishnamurthy and R. Taylor (1985), *AIChE J.*, 31, 449-456.

3. R. Krishnamurthy and R. Taylor (1985), *AIChE J.*, 31, 456-465.

4. R. Krishnamurthy and R. Taylor (1985), *AIChE J.*, 31, 1973-1985.

5. H. R. Mortaheb, Y. Iimuro, H. Kosuge and K. Asano (2000), J. Chem. Eng. Japan, 33, 597-604.

6. H. R. Mortaheb, H. Kosuge and K. Asano (2001), J. Chem. Eng. Japan, 34, 493-500.

7. H. Kosuge and K. Asano (1982), J. Chem. Eng. Japan, 15, 268-273.

8. AIChE Research Committee (1958), Bubble Tray Design Manual, AIChE, New York.

9. J. Gmehling and U. Onken (1977), Vapor-Liquid Equilibrium Data Collection, Vol. 1, Part 2a, DECHEMA, Frankfurt.

10. R. C. Reid, J. M. Prausnitz and B. E. Poling (1987), The Properties of Gases and Liquids, 4th ed., McGraw-Hill, New York.

11. P. B. Cairns and I. A. Furzer (1990), Ind. Eng. Chem. Res., 29, 1364-1382.

12. H. R. Mortaheb (2002), Analysis of Separation Performance of Sieve Tray Columns in Heterogeneous Distillation Based on Mass Transfer Model, PhD Thesis, Tokyo Institute of Technology, Japan.

Key Words:
Heterogeneous Azeotropic Distillation, Sieve Tray, Non-equilibrium Stage Model, Simulation, Dehydration Process